A SIMULATION-BASED ANALYSIS OF SUBSYNCHRONOUS RESONANCE WITH TCSC

Sreenadh BATCHU, Shashidhara M KOTIAN, Shubhanga K. N.

Department of Electrical Engineering, National Institute of Technology Karnataka, Surathkal, Srinivasnagar, Mangalore, Karnataka, INDIA – 575025. Phone:+91-9008418124, +91-9449388208
Email: sreenadh10@gmail.com, shashikotian@gmail.com, knsa1234@yahoo.com.

Abstract: *In this paper a time-domain simulation-based SSR analysis has been carried out in PSCAD/EMTDC employing the IEEE first-benchmark system with thyristor-controlled series capacitor (TCSC). Though torsional-mode detuning behavior of a TCSC is well known its tuning performance for certain firing angles is demonstrated employing modal-speed evaluations. An attempt has been made to understand this nature of TCSC by obtaining its frequency response characteristics using frequency scanning technique. From the results it is inferred that the equivalent impedance of TCSC offers fictitious resistive component leading to mode-detuning. However, it is observed that at higher values of firing angle the resistive behavior diminishes thus resulting in mode-tuning.*

Key words*: subsynchronous resonance, frequency response, series compensation, TCSC.*

1. Introduction

In a stability constrained power system, where transmission system expansion is restricted due to limited right-of-way, compensation using fixed series capacitors (FSC) has been the natural choice for improving the power transfer capability of transmission system [1]. However, in such systems there is a possibility of adverse interaction between the generator-turbine mechanical system and the electrical network compensated with fixed series capacitors – known as subsynchronous resonance (SSR) [2]-[6]. From the literature [7]-[12], it is clear that there has been a continued effort to analyze the SSR phenomenon employing various techniques such as eigenvalue analysis, frequency scanning and time-domain techniques to investigate different countermeasures for mitigating the SSR effects. With the development of flexible AC transmission systems (FACTS) there has been a continued effort to provide an effective solution to mitigate SSR [13]-[15]. Extensive studies both on computer simulations and field investigations [16]-[18], showed that a thyristor controlled series capacitor (TCSC) can reduce the SSR caused by a conventional fixed series capacitor and is generally used as a top-up with respect to a FSC compensation.

It is well known that the eigenvalue analysis of SSR with just FSC itself is not straight forward since it requires detailed modeling of network transients in addition to other components and controllers. Whereas with TCSC such an analysis is much more complex [19]-[21] as it involves the modeling of thyristor devices and there has been a continued effort to evolve other techniques such as dynamic phasor models [22] and discrete-time models [23]. Under these circumstances, a detailed time-domain simulation-based analysis offers better insight into the SSR behavior of power system with TCSC [18, 23].

Encouraged by these observations the following study results are presented in this paper. To begin with an eigen-analysis of the IEEE first-benchmark system (FBS) for SSR study [24] has been done with FSC. Understanding difficulty in obtaining a linear model of TCSC, a simulation-based analysis is presented using the detailed modeling of TCSC. A simulation-based frequency response analysis of TCSC [25, 26] has been carried out to understand the SSR performance of the system with TCSC with regard to its firing angle and device rating. All simulations are performed on PSCAD/EMTDC [27].

2. The IEEE first-benchmark system

Fig. 1 shows the IEEE FBS used in the SSR analysis [24]. This system is characterized by many torsional modes that are distributed in a relatively wide frequency range in addition to the swing mode.

The electrical and mechanical systems are modeled in PSCAD/EMTDC. The generator is represented by

synchronous machine master library component. Two damper windings are provided in the *q* axis while in the *d* axis one damper and field winding are considered. The mechanical system is represented by a multi-mass spring-dashpot system, with six lumped masses coupled by shaft sections of known torsional elasticity. The complete electrical and mechanical data for the studied system are presented in [24], with mechanical damping being considered as specified in [6]. The generator is provided with a single-time-constant static exciter which is equipped with a Delta-P-Omega PSS (see Appendix for exciter and PSS parameters).

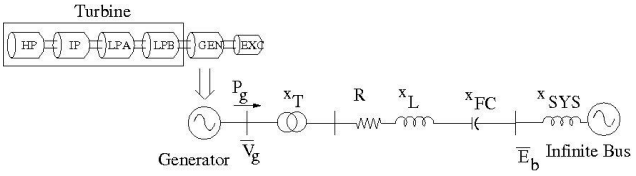

Fig. 1. IEEE first-benchmark system.

2.1. Case studies with fixed compensation levels

A MATLAB-based eigenvalue program is used in the assessment of the dynamic characteristics of the system for FSC. Since there are six rotor masses, the IEEE FBS has five torsional modes. Each of the torsional modes has its largest SSR interaction at a certain value of the series compensation level x_{FC}. This means that torsional interaction is a discrete event. Therefore, any compensation level can be used unless the network subsynchronous mode coincides with any of the torsional mode frequency. By repeated runs of the eigenvalue programme with different x_{FC}, the level of series compensation associated with the maximum torsional interaction for a given mode is determined. The results are tabulated in Table 1 for all torsional modes. It is noted that torsional mode- 5 damping remains unaltered due to its high value of modal inertia [6] indicating that mode-5 cannot be controlled by any means.

Table 1: Frequency of torsional modes and the capacitive reactance for the maximum torsional interaction.

Mode	Frequency (Hz)	x_{FC} (pu)
Torsional mode-4	32.285	0.18
Torsional mode-3	25.54	0.29
Torsional mode-2	20.21	0.38
Torsional mode-1	15.74	0.44

A partial eigenvalue listing is presented in Table 2 for two compensation levels: x_{FC} = 0.35 and x_{FC} = 0.29. As can be seen from the table, x_{FC} = 0.35 leads to a stable operation whereas for x_{FC} = 0.29 torsional mode-3 becomes unstable -see Table 1.

Table 2: Eigenvalues for the IEEE FBS with FSC only.

x_{FC} = 0.35	x_{FC} = 0.29	Comments
-4.6311±j616.63	-4.6155±j595.11	Supersynchronous mode
-3.1001±j136.75	-4.6744±j159.09	Subsynchronous mode
-0.6233±j160.31	0.7031±j160.05	Torsional mode-3

While presenting the corresponding time-domain simulation run it is found that the following difficulties are generally faced:

- The stability inferences made out of the eigenvalue analysis about any particular mode is very difficult to infer from the time-domain simulation as a time-domain response is generally made up of many modes associated with the system.
- As an extension to the determination of eigenvalues, the participation factor -based analysis provides information about a dominant state variable with respect to a mode and observing which in the time-domain simulation, the stability information of that particular mode can be inferred. However, such an analysis is found to be effective in the power swing (i.e., mode-0) oscillation studies and they fail in the analysis of the stiff systems such as SSR studies especially when multiple modes are unstable.

In this connection, the mode identification using modal-speed calculation [28] is found to be very effective in time-domain simulations. Further, the modal speed deviation can also be used as a control signal for the supplementary controllers to damp the torsional oscillations [29, 30].

In an effort to calculate the modal speed in the simulation responses, the modal speed deviation $\Delta\omega_{Ml}$ corresponding to the mode l is approximately obtained as follows:

$$\Delta\omega_{Ml} = v_l^T [\Delta\omega_{HP}, \Delta\omega_{IP}, \ldots \Delta\omega_{EXC}]^T \quad (1)$$

Where, v_l^T is a vector containing the left eigenvector components corresponding to individual angular speed deviations of the rotor masses of the turbine-generator system ($\Delta\omega_{HP}$, $\Delta\omega_{IP}$, ... $\Delta\omega_{EXC}$). It is to be noted that these eigenvectors are obtained

corresponding to the unconnected mechanical system neglecting damping.

For the case in hand, the time-domain simulation is started initially with generator as a voltage source and then the power is ramped up to the required level i.e., to P_g =1.0, and then the generator-turbine system are switched at 3 s. A test disturbance in the form of a step change in the mechanical power of all the turbines, is applied at t = 3.5 s. The deviations in modal speeds for the case x_{FC} = 0.29 are as shown in Fig. 2. In the figure, the growing oscillations clearly indicate the instability of mode-3.

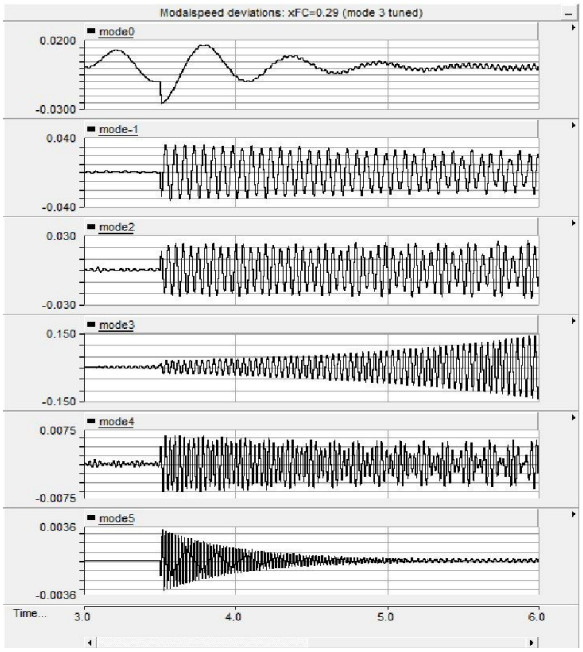

Fig. 2. Modal speed deviations for x_{FC} = 0.29.

2.2. Time-domain simulation with TCSC

The basic structure of a TCSC is a thyristor controlled reactor (TCR) in parallel with a fixed capacitor, as shown in Fig. 3.

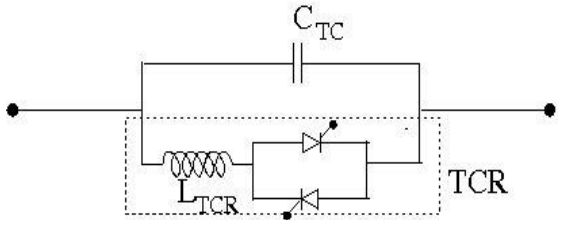

Fig. 3. Schematic diagram of a TCSC module.

In a practical TCSC implementation, several such basic modules may be connected in series to obtain the desired voltage rating and operating characteristics. The TCSC combination allows the fundamental frequency capacitive reactance to be smoothly controlled over a wide range by just adjusting the firing angle of the bi-directional thyristor pairs [14, 21] in the vernier capacitive range [6].

2.2.1. Fundamental- frequency TCSC characteristics

The characteristic of the TCSC main circuit depends on the relative reactances of the capacitor bank $x_{TC} = \frac{1}{\omega C_{TC}}$ and the thyristor branch x_{TCR} $=\omega L_{TCR}$. The resonant frequency ω_r of the LC-circuit formed by the inductance in the thyristor branch and the capacitance in the series capacitor bank is given by

$$\omega_r = \frac{1}{\sqrt{L_{TCR} C_{TC}}} = \omega_0 \sqrt{\frac{x_{TC}}{x_{TCR}}} \qquad (2)$$

Assuming that the line current is sinusoidal, the equivalent reactance offered by the TCSC at the fundamental frequency can be represented as a variable reactance x_{TCSC}. There exists a steady-state relationship between the firing angle α (measured with respect to the positive zero-crossing of the capacitor voltage) and the reactance x_{TCSC} which can be described by the following equation [6]

$$x_{TCSC} = x_{TC} - \frac{{x_{TC}}^2}{(x_{TC} - x_{TCR})} \frac{(2\beta + \sin 2\beta)}{\pi} + \frac{4{x_{TC}}^2}{(x_{TC} - x_{TCR})} \frac{\cos^2 \beta}{(K^2 - 1)} \frac{(K \tan K\beta - \tan \beta)}{\pi} \qquad (3)$$

Where β represents the half of the conduction angle and is related to α as

$$\beta = \pi - \alpha \qquad (4)$$

It is customary to define boost factor, B_f, as the ratio between the x_{TCSC} and x_{TC} as

$$B_f = \frac{x_{TCSC}}{x_{TC}} \qquad (5)$$

Of many other modes of operation of TCSC [6], in the present application only the capacitive vernier mode of operation is implemented. In this operating mode, the thyristor valves are gated in the region of $\alpha_{min} < \alpha < 180^o$ such that the effective value of TCSC reactance is in the capacitive region. In this range x_{TCSC} increases as α is reduced below 180^o and is maximum for $\alpha = \alpha_{min}$ (which may correspond to x_{TCSC} equal to be 3 times x_{TC}). α_{min} is above a value of α which corresponding to the parallel resonance of TCR and the capacitor (at fundamental frequency)

denoted as α_{res}. The angle corresponding to resonance depends on the choice of K which is defined as the quotient between the resonant frequency ω_r and network nominal frequency ω_0 as

$$K = \frac{\omega_r}{\omega_0} = \sqrt{\frac{x_{TC}}{x_{TCR}}} \qquad (6)$$

Reasonable values of K fall in the range of 2 to 3 [31, 32]. Table 3 summarizes the variation of α_{res} for different values of K.

Table 3: Effect of K on α resonance.

K	1.5	2	2.5	3
$\beta res = \frac{90}{K}$	60^o	45^o	36^o	30^o
$\alpha res = 180 - \beta res$	120^o	135^o	144^o	150^o

The variation of B_f as a function of α is shown in Fig. 4 for two different values of K in the capacitive vernier region.

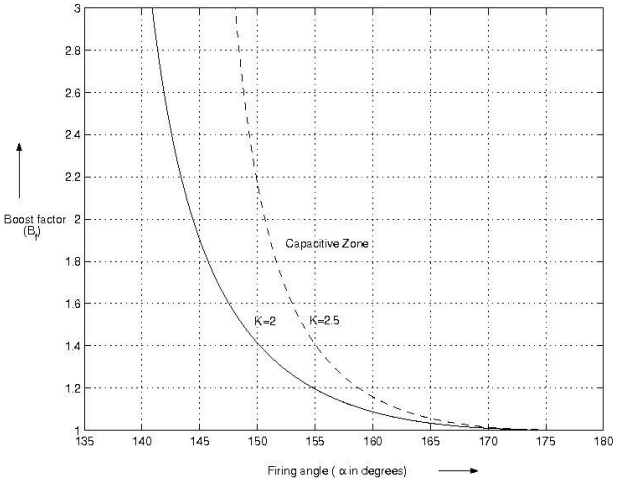

Fig.4. Boost factor vs α

2.2.2. Case studies with constant reactance-control for TCSC

A TCSC device operating with an open-loop constant reactance-controller is considered to substitute for a portion of the FSC compensation in the IEEE FBS. The system is modified as shown in Fig. 5. For a given x_{TC} and α setting, the device offers a reactance x_{TCSC} as per Fig. 4.

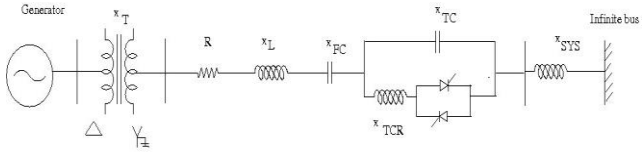

Fig. 5.IEEE FBS system with a TCSC.

A TCSC with x_{TC} = 0.1 and K=2 is chosen for this case study. In all cases x_{FC} is adjusted so that x_{FC} + x_{TCSC} = 0.29 for any firing angle we choose. Now TCSC is operated with a firing angle order of α = 159.22^o which corresponds to a boost factor, B_f =1.1. From Fig. 6 it can be seen that mode-3 (which was unstable when x_{FC} = 0.29 with only FSC compensation -see Fig. 2), is now stable due to the presence of TCSC even for the same effective capacitive compensation. This case demonstrates that TCSC when used as top-up compensation with respect to FSC can remove the possibility of torsional interaction with respect to mode-3. However, it is found that when TCSC firing angle is increased to α =170.92^o which corresponds to a boost factor of B_f =1.007, the system becomes unstable exciting mode-3 -see Fig. 7.

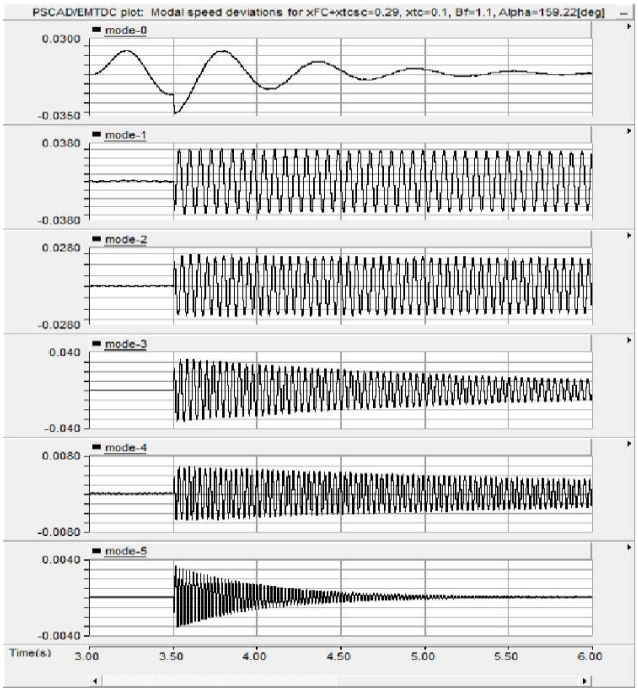

Fig. 6. Modal speed deviations for x_{FC} + x_{TCSC} = 0.29, x_{TC} = 0.1 and α =159.22^o.

The above case study has been repeated with x_{TC} = 0.25 for a firing angle of α = 170.92^o. From Fig. 8 it can be seen that the system is now stable.

A number of such simulations are carried out in PSCAD/EMTDC for different firing angles. Results are summarized in Table 4. From the table it is concluded that a TCSC operating under constant reactance-control offers a greater level of immunity to torsional interaction at higher device ratings. However, this may lead to increased cost of TCSC systems.

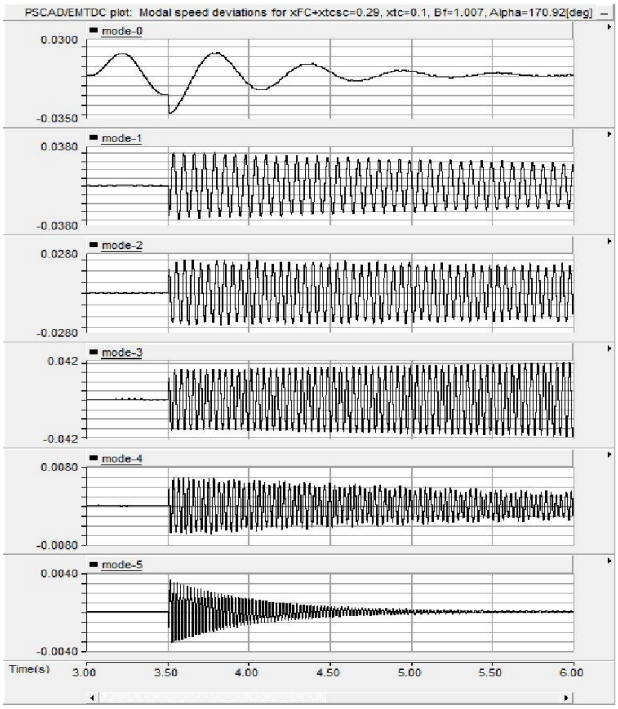

Fig. 7. Modal speed deviations for $x_{FC} + x_{TCSC} = 0.29$, $x_{TC} = 0.1$ and $\alpha = 170.92^{o}$.

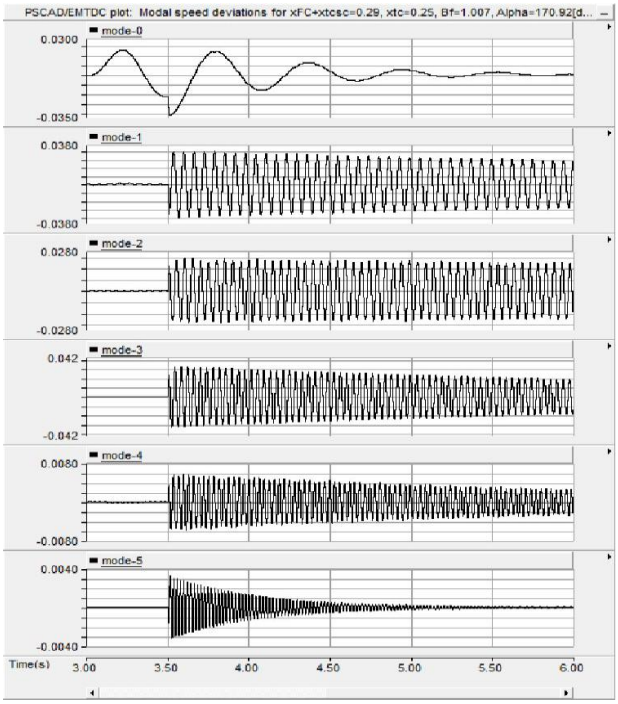

Fig. 8. Modal speed deviations for $x_{FC} + x_{TCSC} = 0.29$, $x_{TC} = 0.25$ and $\alpha = 170.92^{o}$.

3. Frequency response analysis of TCSC

In previous section it is observed that a TCSC operating in the capacitive vernier mode offers a way to effectively mitigate the SSR problem. It is also noticed that such a performance of TCSC depends on the rating of TCSC and the firing angle of the constant reactance controller. There has been many attempts in the literature to understand this behaviour of TCSC using frequency response analysis [18] and discrete-time modelling of TCSC [23, 33]. Though the discrete-time modelling approach is accurate, it is highly complex as it involves the discretization of the complete system.

Table 4: Parametric variation of TCSC with $x_{FC} + x_{TCSC} = 0.29$.

x_{TC}	B_f	α	x_{TCSC}	x_{FC}	Stability inference
0.10	1.10	159.22	0.1100	0.1800	stable
	1.05	163.08	0.1050	0.1850	stable
	1.02	167.27	0.1020	0.1880	stable
	1.01	169.81	0.1010	0.1890	unstable
	1.007	170.92	0.1007	0.1893	unstable
0.25	1.10	159.22	0.2750	0.0150	stable
	1.05	163.08	0.2625	0.0275	stable
	1.02	167.27	0.2550	0.0350	stable
	1.01	169.81	0.2525	0.0375	stable
	1.007	170.92	0.2518	0.0382	stable

In this paper an attempt has been made to explain the behaviour of TCSC by using frequency response analysis [25, 26]. Because of the specific switching pattern of a TCSC device its operation can be considered to include both discrete and continuous characteristics and therefore determination of sub and supersynchronous frequency response of the device is not a straightforward task. Therefore, frequency response curves of TCSC are obtained by employing time-domain based frequency scanning (FS) method [34] using PSCAD/EMTDC. Frequency response is obtained over the network frequency range of 10 Hz to 100 Hz. The main objective of this study is to evaluate the equivalent impedance offered by a TCSC for different frequencies. Fig. 9 depicts the adopted scheme.

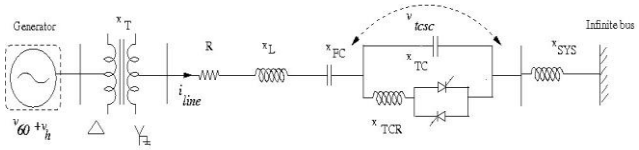

Fig. 9. System configuration for obtaining the TCSC equivalent impedance.

The procedure listed in [34] is adopted to determine the frequency response of TCSC. Assuming the synchronous machine to be a voltage source a disturbance signal, v_h , with particular frequency is added to the fundamental components.

Then the instantaneous values of the voltage across the TCSC, v_{TCSC}, and line current, i_{line}, are measured. Having extracted the magnitude and angle information at the disturbance signal frequency, the ratio between the phasor voltage and current per phase provides the necessary TCSC equivalent impedance, Z_{TCSC} at that frequency. The real and imaginary components of this impedance value are plotted against network frequency to draw conclusions. Here, capacitive reactance is treated as a positive quantity.

3.1. Frequency response analysis - case studies

The following case studies are carried out

1. Frequency response for different firing angle.
2. Frequency response for different device rating.

3.1.1. Frequency response for different firing angle

Using the FS technique described above, the equivalent impedances of a TCSC with x_{TC} = 0.1 and K= 2 for α = 159.22^o and α = 170.92^o are obtained in the frequency range corresponding to torsional frequencies. It is to be noted that for a network frequency component of f_{er}, a torsional mode having frequency ($f_0 - f_{er}$) may have the maximum interaction. For example, if f_{er}=35 Hz it influences the torsional mode having frequency 60-35 = 25 Hz, i.e., torsional mode-3 in the IEEE FBS. The real and imaginary components of Z_{TCSC} are drawn with respect to f_{er} and are shown in Fig. 10. A close look at the figure shows that the reactance of the TCSC at nominal frequency is identical to that shown in Table 4.. Further, it is interesting to see that TCSC offers a nonzero and positive resistance in subsynchronous frequency range [26]. It should be noted that while modelling the TCSC no explicit resistive elements are used, i.e., the device is assumed to be lossless. Thus, this fictitious resistive component of Z_{TCSC} is imagined to offer damping for torsional modes. A relatively higher resistance offered by the TCSC at 35 Hz for α = 159.22^o can be expected to provide additional damping for the torsional mode-3. The time-domain simulation presented in Fig. 6 confirms this inference. However, at α = 170.92^o, the resistance offered by the TCSC is relatively small so that an insufficient damping presents a potential risk of tuning torsional interactions. This was confirmed already by the time-domain simulations -see Fig. 7. In addition, the resistance of the TCSC which is entirely a positive number for all frequency range drops to zero at 60 Hz.

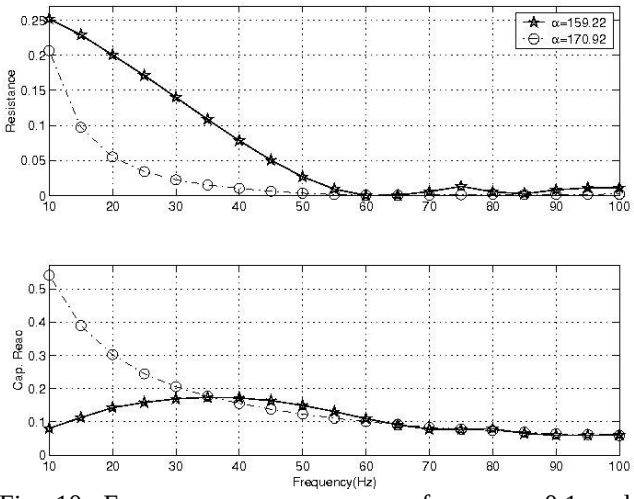

Fig. 10. Frequency response curves for x_{TC} = 0.1 and different firing angles.

3.1.2,. Frequency response for different device ratings

In this case Z_{TCSC} plots are obtained for different TCSC device ratings, x_{TC} . Fig. 11 shows the frequency response curves for various device ratings for α = 159.22^o. It is interesting to note that with an increase in device rating, resistance offered by the device at subsynchronous frequencies increases offering more damping.

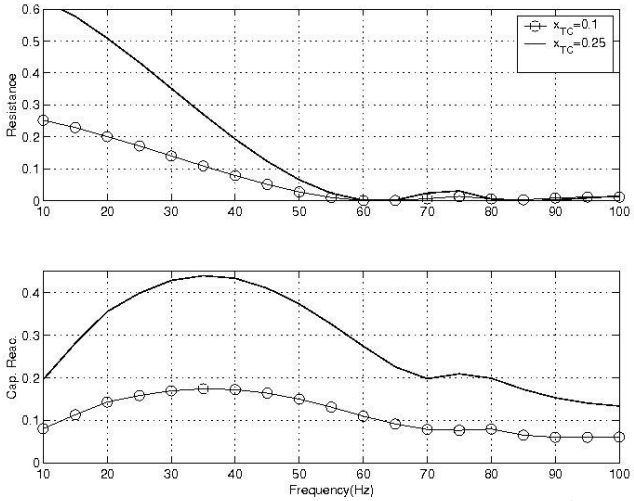

Fig. 11. Frequency response curves for α = 159.22^o and different x_{TC}.

The above study is repeated for α = 170.92^o and the corresponding Z_{TCSC} plots are shown in Fig. 12. From the figure it can be seen that for the chosen angle with x_{TC}= 0.25 the TCSC offers relatively more

resistive component than in a case when x_{TC}=0.1. This inference, to some extent, explains the reason for no mode-3 interaction with higher rating of the device for higher values of α (compare Figs. 7 and 8).

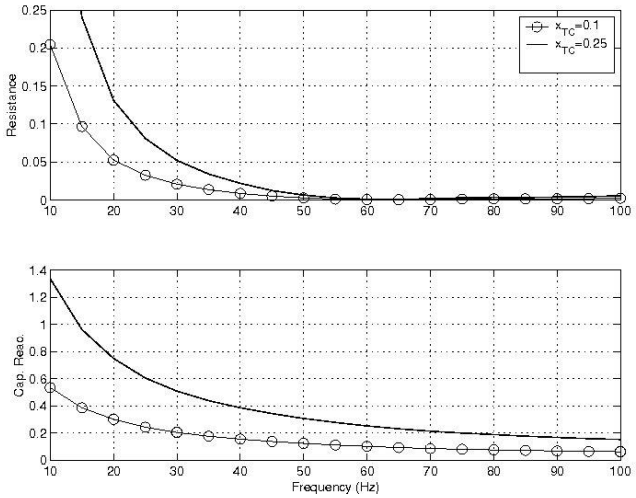

Fig. 12. Frequency response curves for α = 170.92^o and different x_{TC}.

From the above frequency response analysis the following observations were made:

- At fundamental frequency the device impedance is purely capacitive, at subsynchronous frequencies it possesses considerable resistive component whereas at supersynchronous frequencies the resistive value is negligibly small.
- For a given value of x_{TC}, the TCSC resistive behaviour increases as we move away from 180^o.
- For a given α, the resistive behaviour of TCSC increases with device ratings. However, higher device ratings are generally not chosen as it is not economical. To overcome the problem of torsional interactions with low device ratings for higher α is generally handled by employing a subsynchronous resonance damping controller [33].

4. Conclusions

In this paper simulation-based SSR analysis is presented with the IEEE FBS employing PSCAD/EMTDC for both fixed and variable series compensation. A full-fledged model of TCSC is included in the system and the effects of firing angle on the modal interactions are demonstrated for different device ratings. Employing frequency scanning technique, frequency response curves of TCSC are obtained using which reasoning is made to explain the SSR behavior of the system with TCSC.

5. Appendix : Test system data and operating conditions

5.1. System operating condition

P_g=1.0, V_g=1.0, E_b=1.0

5.2. Exciter data

Single-time-constant static exciter is with K_A=200, T_A=0.025 s.

5.3. Delta-P-Omega PSS data

The Delta-P-Omega PSS uses a phase lead circuit (with center frequency f_m=2.37 Hz and angle lead Φ_m=22.29^o) with gain set to K_s=1.25 so that the swing-mode damping factor is about 5% for FSC compensation of x_{FC}=0.3.

References

1. Kimbark E. W.: *Improvement of system stability by switched series capacitors.* In: IEEE Trans. Power App. Syst., Vol. 85, No.2, Feb. 1966, p. 180-188.

2. Kilgore L. A., Elliott L. C. and Taylor E. R.: *The prediction and control of self-excited oscillations due to series capacitors in power systems*. In: IEEE Trans. Power App. Syst., Vol. 90, No.3, May/June 1971, p. 1305-1311.

3. Balance J. W. and Goldberg S.: *Subsynchronous resonance in series compensated transmission lines.* In: IEEE Trans. Power App. Syst., Vol. 92, No. 5, Sep./Oct. 1973, p. 1649-1658.

4. Anderson P. M., Agrawal B. L., and Van Ness J. E.: *Subsynchronous Resonance in Power Systems*. IEEE Press, New York, 1990.

5. IEEE Committee Report: *Reader's guide to subsynchronous Resonance*. In: IEEE Trans. Power Syst., Vol. 7, No. 1, Feb. 1992, p. 150-157.

6. Padiyar K.R.: *Analysis Of Subsynchronous Resonance in Power Systems*. Kluwer Academic Publishers, Norwell, MA , 1999.

7. Kimbark E. W.: *How to improve system stability without risking subsynchronous resonance*. In: IEEE Trans. Power App. Syst., Vol. 96, No. 5, Sep/Oct. 1977, p. 1608-1619.

8. Agrawal B. L. and Farmer R. G.: *Use of frequency scanning techniques for subsynchronous resonance analysis.* In: IEEE Trans. Power App. Syst., Vol. 98, No. 2, Mar/Apr. 1979, p. 341-349.

9. IEEE SSR Working Group: *Countermeasures to subsynchronous resonance problems*. In: IEEE Trans. Power App. Syst., Vol. 99, Sep. 1980, p. 1810- 1818.

10. Larsen E.V. and Baker D.H.: *Series compensation operating limits - a new concept for subsynchronous resonance stability analysis.* In: IEEE Trans. Power App. Syst., Vol. 99, No. 5, Sep/Oct. 1980, p. 1855-1863.

11. IEEE Committee Report: *Terms, definitions and symbols for subsynchronous oscillations*. In: IEEE Trans. Power App. Syst., Vol. 104, No. 6, June 1985, p. 1326-1334.
12. Baker D. H., Boukarim G. E., Aquila R. D. and Piwko R. J.: *Subsynchronous resonance studies and mitigation methods for series capacitor applications*. In: Proceedings of the IEEE PES Conf. and Exp., Durban, South Africa, July 2005, p. 386-392.
13. Song Y. H. and Johns A. T.: *Flexible AC Transmission Systems (FACTS)*. IEE Press, London, UK, 1999.
14. Hingorani N. G. and Gyugyi L.: *Understanding FACTS*. IEEE Press, New York, 2000.
15. Mathur R. M. and Varma R. K.: *Thyristor-Based FACTS Controllers for Electrical Transmission Systems*. IEEE Press, New York, 2002.
16. Zhu W., Spee R., Mohler R.R., Alexander G.C., Mittelstadt W.A. and Maratukulam D.: *An EMTP study of SSR mitigation using the thyristor-controlled series capacitor*. In: IEEE Trans. Power Delivery, Vol. 10, No. 3, Jul. 1995, p. 1479-1485.
17. Piwko R.J., Wegner C.A., Kinney S.J. and Eden J.D.: *Subsynchronous resonance performance tests of the Slatt thyristor-controlled series capacitor*. In: IEEE Trans. Power Delivery, Vol. 11, No. 2, Apr. 1996, p. 1112-1119.
18. Pilotto L. A. S., Bianco A., Long F. W. and Edris A. A.: *Impact of TCSC control methodologies on subsynchronous resonance oscillations*. In: IEEE Trans. Power Delivery, Vol. 18, No. 1, Jan. 2003, p. 243-252.
19. Othman H.A. and Angquist L.: *Analytical modelling of thyristor controlled series capacitors for SSR studies*. In: IEEE Trans. Power Syst., Vol. 11, No. 1, Feb. 1996, p. 119-127.
20. Jayaram Kumar S.V., Arindam Ghosh and Sachchidanand: *Damping of subsynchronous resonance oscillations with TCSC and PSS and their control interaction*. In: Elect. Power Syst. Res., Vol. 54, July 2000, p. 29-36.
21. Padiyar K. R.: *FACTS Controllers in Power Transmission and Distribution*. New Age Int ., New Delhi, India., 2009.
22. Mattaveli P., Verghese G. C., and Stankovic A. M.: *Phasor dynamics of thyristor-controlled series capacitor systems*. In: IEEE Trans. Power Syst., Vol. 12, No. 3, Aug. 1997, p. 1259-1266.
23. Joshi S. R. and Kulkarni A. M.: *Analysis of SSR performance of TCSC control schemes Using a modular high bandwidth discrete-time dynamic model*. In: IEEE Trans. Power Syst., Vol. 24, No. 2, May 2009, p. 840-848.
24. IEEE SSR Task Force: *First benchmark model for computer simulation of subsynchronous resonance*. In: IEEE Trans. Power App. Syst., Vol. 96, No. 5, Sep./Oct. 1977, p. 1565-1572.
25. Daneshpooy A. and Gole A. M.:*Frequency response of the thyristor controlled series capacitor*. In: IEEE Trans. Power Delivery, Vol. 16, No. 1, Jan. 2001, p. 53-58.
26. Kabiri K., Henschel S. and Dommel H. W.: *Resistive behavior of thyristor-controlled series capacitors at subsynchronous frequencies*. In: IEEE Trans. Power Delivery, Vol. 19, No. 1, Jan. 2004, p. 374-379.
27. Digital Simulation Software Package, PSCAD/EMTDC, Version V4.0.
28. Jennings G. D., Harley R. G. and Levy D. C.: *Sensitivity of subsynchronous resonance predictions to turbo-generator modal parameter values and to omitting certain active subsynchronous modes*. In: IEEE Trans. Energy Conversion, Vol. 2, No. 3, Sep. 1987, p. 470-479.
29. Wasynczuk O.: *Damping subsynchronous resonance using reactive power control.* In: IEEE Trans. Power App. Syst., Vol. 100, No. 3, Mar. 1981, p. 1096-1104.
30. Jusan F. C., Gomes S. and Taranto G. N.: *SSR results obtained with adynamic phasor model of SVC using modal analysis*. In: Int. J. Elect. Power Energy Syst., Vol. 32, No. 6, Jul. 2010, p. 571-582.
31. Zheng Xu, Guibin Zhang and Haifeng Liu: *The Controllable Impedance Range of TCSC and its TCR Reactance Contraints*. In: Proceedings of the IEEE Power Engineering Society Summer Meeting, July 2001, p. 939-943.
32. Meikandasivam S., Nema R. K., and Jain .K.: *Selection of TCSC parameters: capacitor and inductor*. In: Proceedings of the Int. Conf. Power Elect. (IICPE), 2010, p. 1-5.
33. Joshi S. R., Cheriyan E. P. and Kulkarni A. M.: *Output feedback SSR damping controller design based on modular discrete-time dynamic model of TCSC*. In: IET Gener. Transm. Distrib. , Vol. 3, No. 6, 2009, p. 561-573.
34. Jiang X. and Gole A.M.: *Frequency scanning method for the identification of harmonic instabilities in HVDC system.* In:IEEE Trans.Power Delivery, Vol.10, Oct. 1995, p.1875-1881.